

Moisture effects on the toughness, mode-I and mode-II of particles filled quasi-isotropic glass–fibre reinforced polyester resin composites

V. K. SRIVASTAVA*, P. J. HOGG

*Department of Materials, Queen Mary & Westfield College, University of London,
Mile End Road, London, E1 4NS, UK
E-mail: vijayks@banaras.ernet.in*

An experimental programme is presented for the effect of moisture on the toughness, mode-I and mode-II of aluminium tri-hydrate and polyethylene filled and unfilled quasi-isotropic glass–fibre reinforced epoxy–vinylester resin (GFRP) composites. Specimens were exposed in water at room temperature (20 °C) for a period of 8 months and the effect of moisture content on toughness, G_{Ic} and G_{IIc} values were obtained at an interval of every 2 months. Some samples were exposed in hot water at 40 °C temperature to accelerate the uptake of moisture and produce saturated composites. The results indicate that equilibrium moisture content and diffusion coefficients increase with increase of weight of filler content in GFRP composites which is linked to an increase in microscopic cracking. Also mode-I, toughness of all composites increased with an increase in moisture uptake, mode-II toughness was relatively unaffected. Aluminium-tri-hydrate filled GFRP composites showed a higher moisture uptake, which resulted in higher values of both mode-I and mode-II, toughness than the polyethylene filled and unfilled GFRP composites. © 1998 Chapman & Hall

1. Introduction

Resin matrix composite materials have been used extensively in various industries over the past several decades. Often, the environment in which composites are used determines their mechanical performance. The combined influence of moisture and thermal environments can significantly degrade the compressive strength of epoxy-based composites and these factors must be understood when designing structures made from composite materials. This degradation can take the form of change to the fibres and matrix or a weakening of the fibre/matrix interface. Moisture absorption by the composite may remove resin material or expand the matrix causing microcracking to develop along with plasticization. These hydrothermal effects can also reduce the glass transition temperature of the resin and may increase the dimensions and tolerance of the materials [1]. Hot or wet environments are thought to have a significant role on determining the damage tolerance behaviour of composites and these influences have to be assessed in order to ensure that the performance of a composite is completely characterized for the extremes of environment that may be encountered in service [2].

Most recent work in the literature has been directed toward developing a fracture mechanics methodology for predicting delamination behaviour. Delaminations constitute one of the most frequently encountered defects in exposed composites after service life [3].

Research conducted on moisture absorption by several authors [4–7] indicates that water penetration into polymer matrix composites (PMC) involves three mechanisms: (1) direct diffusion of water molecules into the matrix and, to a much less extent, into the filler material; (2) flow of water molecules along the filler–matrix interface, followed by diffusion into the bulk resin; and (3) transport of water by microcracks or other form of microdamage, such as pores or small channels already present in the material or generated by water attack. Experimental studies have shown that water diffusion into PMCs initially follows the Fickian model, i.e. proportionality between mass gain and the square root of immersion time [6], which corresponds to the first mechanism. The latter two mechanisms as well as dissolution of charged species in liquid films at the filler–matrix interface, have been reported to lead to deviations from Fickian behaviour, such as the non-attainment of equilibrium, a decrease in the mass gain after a maximum water absorption, or double-step sorption kinetics.

An increase in the water salinity leads to a decrease in the maximum water absorption and saturation time for immersed glass and carbon-reinforced epoxies, as well as glass-reinforced polyesters. It is clear that a resin like a polyester will show great resistance to moisture absorption when properly bonded to the glass in a fabric laminate, but when equally well cured as a casting it will swell and rupture [5]. Water

*Also: Department of Mechanical Engineering, Institute of Technology, Banaras Hindu University, Varanasi 221 005, India.

absorbed in the interphase region may actually increase the modulus of the polymer in that region by filling in the sub-microcracks and limiting the yielding response. This action of the resin interphase tends to reduce the composites ability to counteract crack propagation at the glass–resin interface, resulting in a lower ultimate composite strength. Partial water absorption may give strengths somewhat higher than dry strengths. This phenomenon is noted in strengths after 2 h in boiling water for many well-bonded composites [7].

In this study, moisture absorption behaviour in aluminium tri-hydrate filled glass–fibre reinforced polyester resins (GFRP) and polyethylene filled GFRP, with the various filler contents and unfilled GFRP composites were investigated. Specimens of double cantilever beam (DCB) and end notch flexural (ENF) tests were immersed in distilled water at room temperature for more than 8 months. Weight gain, toughness, mode-I and mode-II were measured, while scanning electron microscopy (SEM) was used to investigate the surface modification.

2. Experimental procedure

2.1. Materials

The reinforcing material used was an E-glass fibre quadriaxial fabric (weight 610 gm^{-2} and dry thickness 0.55 mm). The matrix system was an epoxy–vinylester resin (Derakane 411–45. Accelerator-E, 2% by volume of the resin and Catalyst-M, 3% by volume of the resin) supplied by Dow Europe. Polyethylene (average particle size 40 nm) and aluminium tri-hydrate, $\text{Al}(\text{OH})_3$, (average particle size $10 \mu\text{m}$) were used as filler materials.

Laminates, nominally 2.5 mm thick were prepared by hand lay-up at room temperature. The particulate materials, ranging from 5 to 15% by weight of the matrix, were added to the epoxy–vinylester resin before it was applied to the glass fibre cloth, care was taken to avoid agglomeration of the particles. In the following discussion, these materials will be referred to, for convenience as PI-GFRP (polyethylene-filled) and Al-GFRP (Aluminium tri-hydrate-filled). During fabrication of the laminate, the epoxy vinylester resin flowed from the blended resin into the fabric. Teflon (polytetrafluoroethylene, PTFE) film (0.5 mm thick) was also inserted on the mid-plane at one edge of the laminates to provide a starter notch, for interlaminar toughness tests. The laminates were post-cured at 85°C for 12 h, following the manufacturer's recommendations. The final fibre volume fraction of all laminates was about 0.40 based on weight of materials used. Specimens were cut with a water-cooled diamond cutting wheel and dried for 1 h at 100°C prior to environmental conditioning. Three sets of samples were prepared for each type of composites.

2.2. Effect of water absorption

The basis of environmental testing consists of immersing specimens in a liquid, in this case distilled water, at a room temperature 20°C and for a set period of time.

For this purpose of conditioning, two water baths were used, which contained thermostatic temperature controllers. The specimens were all weighed prior to conditioning using an electronic balance accurate to $\pm 0.0001 \text{ g}$. To see the effect of water on laminates, differing periods of environmental exposure times of 2 months, 4 months, 6 months and 8 months were used. Some sets of specimens were immersed in hot water at a temperature of 40°C to achieve an equilibrium water absorption level in a shorter period of time. When the immersion period had been reached for specimens they were removed from the water baths and then dried with filter paper before weighing.

Most of the evidence in the literature suggests that water is absorbed by a bulk diffusion mechanism in the resin and for flat plates the rate of moisture absorption, $\partial M/\partial t$, through the thickness direction (z) can be described by Ficks second law [9]

$$\partial M/\partial t = D\partial^2 M/\partial z^2 \quad (1)$$

where D is known as the diffusion coefficient. It should be remembered that the two main characteristics of Fickian behaviour are: (1) the absorption curve should be linear with the square root of time initially and (2) the moisture content should reach a saturation level (M_s) at large values of time. The analytical solution of Equation 1 is obtained by the method of separation of variables and yields the amount of moisture uptake, which varies with time as

$$M(t) = M_0 + (M_s - M_0)4/h(Dt/\pi)^{1/2} \quad (2)$$

where M_0 is the initial amount of moisture in the solid, M_s is the final amount at equilibrium and h is the laminate's thickness. The diffusivity can be derived by using the value of M for different values of time

$$D = \pi [h/4(M_s - M_0)]^2 [(M_2 - M_1)/(t_2^{1/2} - t_1^{1/2})]^2 \quad (3)$$

If it is considered that $M_0 = 0$, Equation 3 becomes

$$D = \pi (h/4 M_s)^2 [(M_2 - M_1)/(t_2^{1/2} - t_1^{1/2})]^2 \quad (4)$$

The diffusivity D is obtained from the initial slope of the M_s versus $t^{1/2}$ curve, as shown in Fig. 1a and b.

To get a better estimate of the true one-dimensional homogeneous material through thickness coefficient, D_s , we use a correction factor given by Shen and Springer [9]

$$D_s = D(1 + h/w + h/l)^{-2} \quad (5)$$

where, w and l are the specimen width and length.

If the moisture entering the specimen through the "edges", surfaces hw and hl can be neglected, D_s is given as

$$D_s = D \quad (6)$$

The moisture content and diffusivity coefficient, D_s , of each specimens were calculated as a percentage increase over the dry weight before toughness tests. The results are shown in Figs 2 and 3. After conditioning of each sample for the allotted periods, DCB and

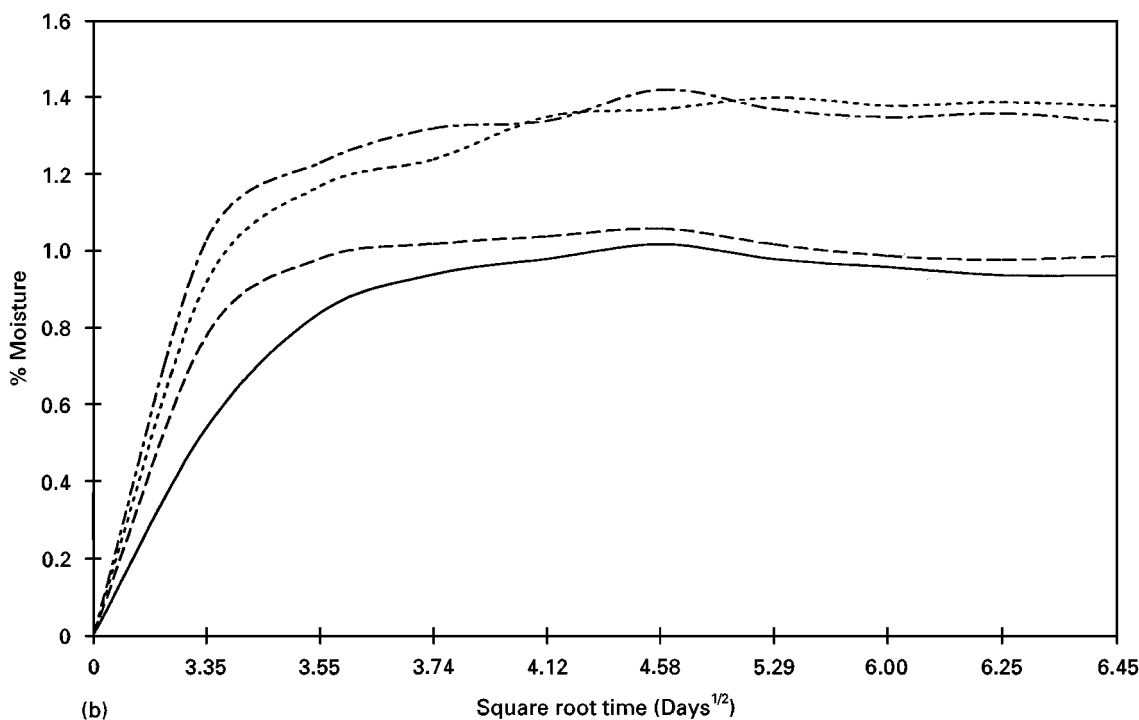
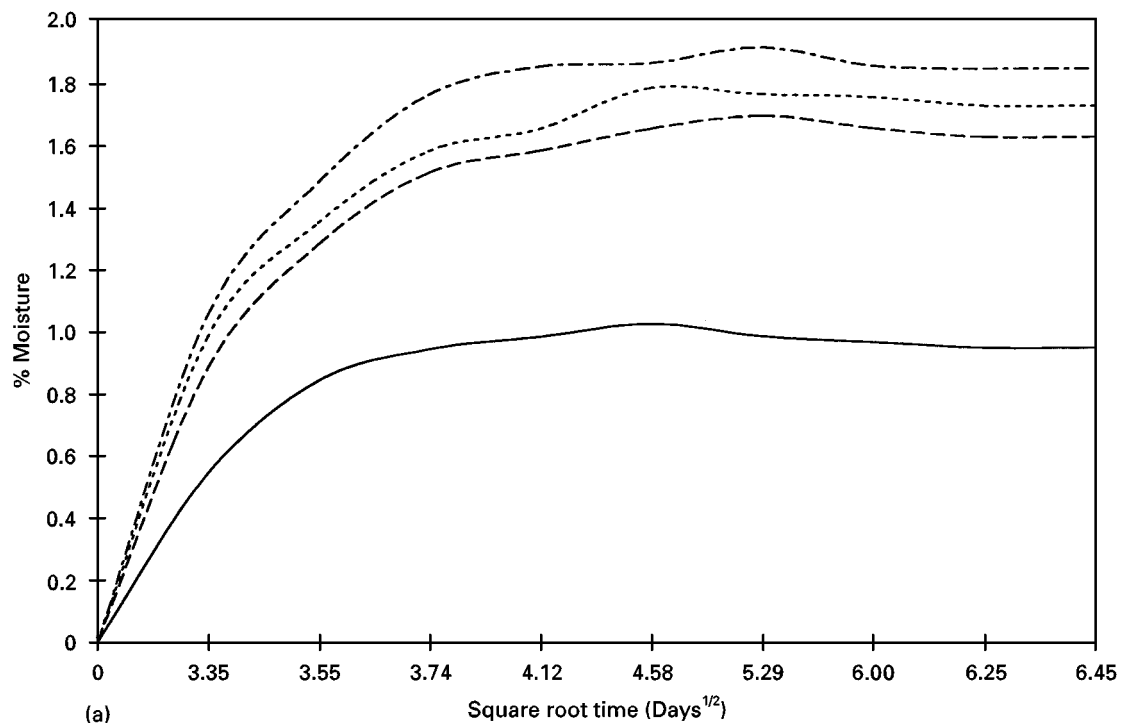


Figure 1 Moisture uptake versus time for (a) GFRP and Al-GFRP composites (—) GFRP; (— — —) 5% Al-GFRP; (— · — ·) 10% Al-GFRP; (- · - ·) 15% Al-GFRP and (b) GFRP and PI-GFRP composites (—) GFRP; (— — —) 5% PI-GFRP; (— · — ·) 10% PI-GFRP; (- · - ·) 15% PI-GFRP.

ENF specimens were loaded for the measurement of toughness in mode-I and mode-II. Also, SEM micrographs were taken before and after the conditioning of unfractured composite samples, as shown in Fig. 4.

2.3. Toughness, mode-I and mode-II tests

2.3.1. Toughness, mode-I test

After environmental testing, steel piano hinges were glued onto the surface of the beam specimens above the notch for application of the load to the specimen during mode-I testing. The sides of the specimen were painted white in order to permit visual crack-tip loca-

tion. The test specimens were loaded in an Instron testing machine, at a crosshead speed of $10 \text{ mm}/\text{min}^{-1}$. One specimen was tested for each condition of material composition and exposure time. The experimental fracture data were recorded in the form of the complete load/displacement curve for all the exposed and unexposed DCB samples as shown in Fig. 5a to g.

From load, displacement and crack length, the strain energy release rate (G_{Ic}) was calculated by using the area method and compliance method [10].

The energy, ΔU , dissipated in the specimen during crack propagation is measured directly from the loading and unloading load-displacement curves in

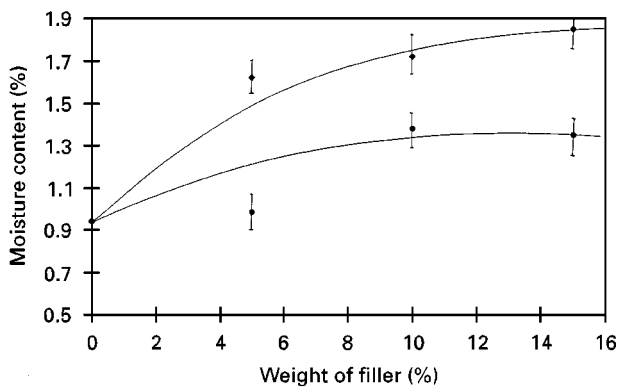


Figure 2 Moisture content versus weight of filler (◆) Al-GFRP; (●) PI-GFRP.

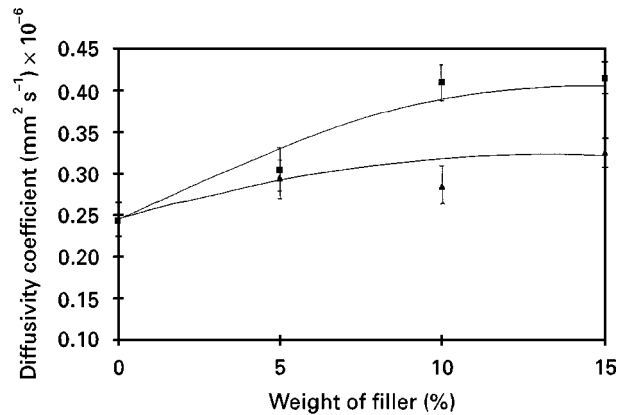


Figure 3 Diffusivity coefficient versus weight of filler (■) Al-GFRP; (▲) PI-GFRP.

a DCB test, and the increment, Δa , of new crack length. The formula for calculation of G_{Ic} is

$$G_{Ic} = \Delta U / W \Delta a \quad (7)$$

By this method a toughness value at each increment of crack growth during propagation was established. An average G_{Ic} value may be obtained from a series of loading and unloading curves, as shown in Fig. 6.

Also, from load–displacement and crack length, the strain energy release rate, G_{Ic} , was obtained using the formula

$$G_{Ic} = 3P_m \delta_m / 2Wa \quad (8)$$

where P_m and δ_m are the peak load and displacement and a is the crack length.

2.3.2. Toughness, mode-II test

The end-notch flexure (ENF) fracture test was used to measure mode-II delamination resistance. This is a three-point bend test in which the specimen contains a precrack. The specimen is placed in such a way that the crack tip is midway between the loading roller and the outer support. The load is applied as controlled displacement (displacement rate 20 mm min^{-1}) and the crack growth is unstable in all cases. During the experiment the curve of load against centre-line deflection was recorded. When the crack starts growing, a sudden load drop is observed and the test is stopped. The maximum recorded load and corresponding displacement is used in the data reduction process.

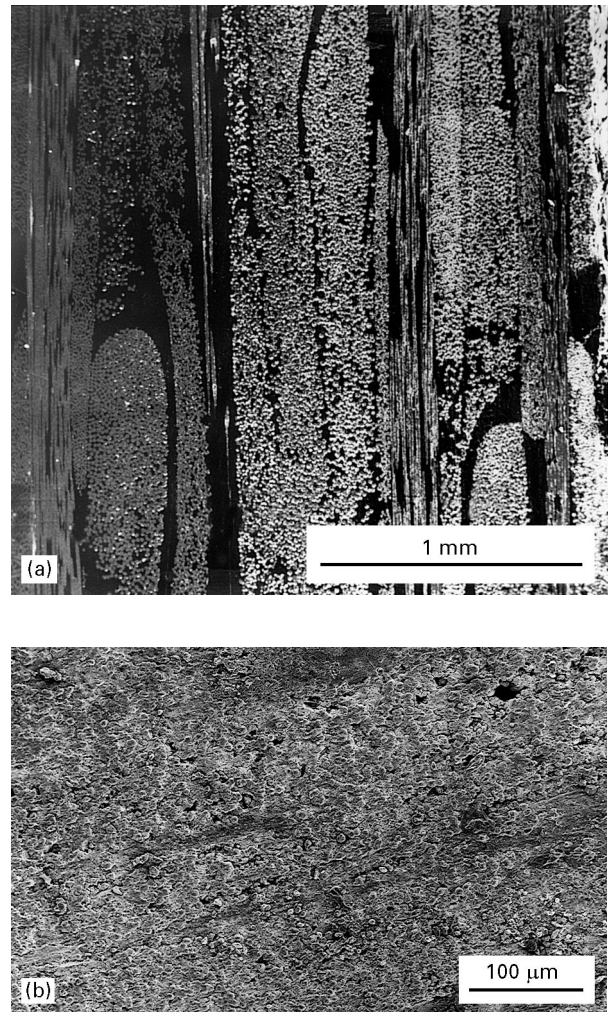


Figure 4 SEM micrograph of unfractured specimens showing (a) the uncracked sample before exposure, (b) the microcracking and voids developed in particle-filled GFRP composites after immersion in water for 120 days at 40°C temperature.

Simple beam theory allows the calculation of the compliance, C , and the critical strain energy release rate can be calculated as [11]

$$G_{Ic} = 9a^2 P_c \delta_c / 2W(2L^3 + 3a^3) \quad (9)$$

where L is the half-span and δ_c is the critical displacement.

3. Results and discussion

3.1. Water absorption

Representative curves for the water uptake by filled and unfilled composites with time in distilled water at 40°C temperature are presented in Fig. 1a and b. The results show that the mass gain at saturation, as well as the time for saturation, increased with increasing filler content. The times to saturation for highly filled composites were very long or complete saturation did not occur within 40 days of immersion at this temperature. For unfilled GFRP composites, the mass gain at saturation was approximately constant after 19 days of immersion.

The slope of the linear part of each curve and saturated moisture content were used to calculate diffusion coefficients which were plotted as a function

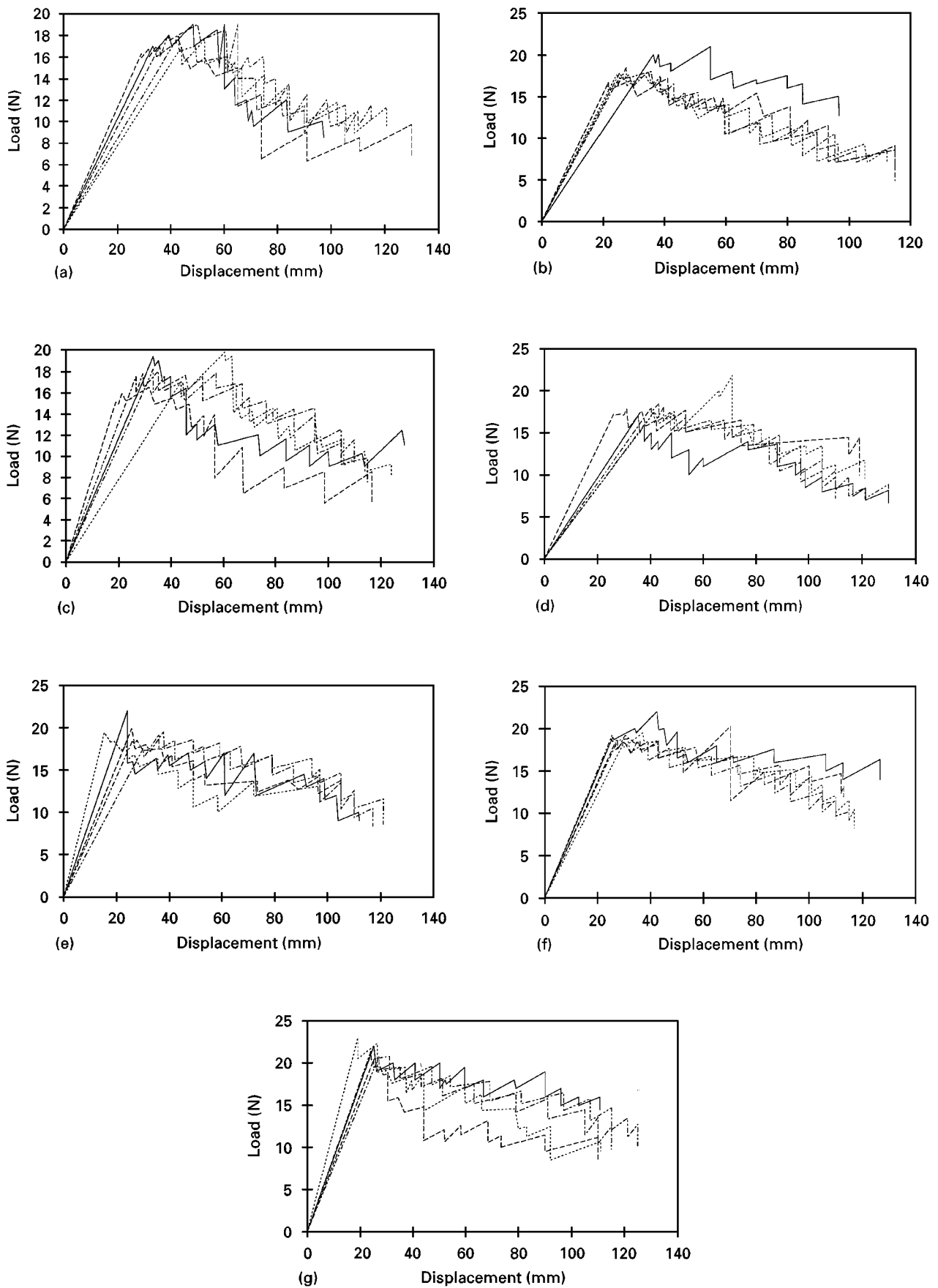


Figure 5 Load–displacement curves for unexposed and exposed in water (a) GFRP composites; (—) $M_s = 0\%$; (---) $M_s = 0.75\%$; (----) $M_s = 0.86\%$; (-----) $M_s = 0.98\%$; (-----) $M_s = 1.08\%$; (b) 5% Al-GFRP (—) $M_s = 0\%$; (---) $M_s = 0.85\%$; (----) $M_s = 0.96\%$; (-----) $M_s = 1.15\%$; (-----) $M_s = 1.24\%$; (c) 10% Al-GFRP (—) $M_s = 0\%$; (---) $M_s = 0.87\%$; (----) $M_s = 1.08\%$; (-----) $M_s = 1.21\%$; (-----) $M_s = 1.34\%$; (d) 15% Al-GFRP (—) $M_s = 0\%$; (---) $M_s = 1.15\%$; (----) $M_s = 1.22\%$; (-----) $M_s = 1.32\%$; (-----) $M_s = 1.45\%$; (e) 5% PI-GFRP (—) $M_s = 0\%$; (---) $M_s = 0.80\%$; (----) $M_s = 0.86\%$; (-----) $M_s = 0.98\%$; (-----) $M_s = 1.12\%$; (f) 10% PI-GFRP (—) $M_s = 0\%$; (---) $M_s = 0.84\%$; (----) $M_s = 0.98\%$; (-----) $M_s = 0.92\%$; (-----) $M_s = 1.15\%$; (g) 15% PI-GFRP (—) $M_s = 0\%$; (---) $M_s = 0.90\%$; (----) $M_s = 1.14\%$; (-----) $M_s = 1.21\%$; (-----) $M_s = 1.28\%$.

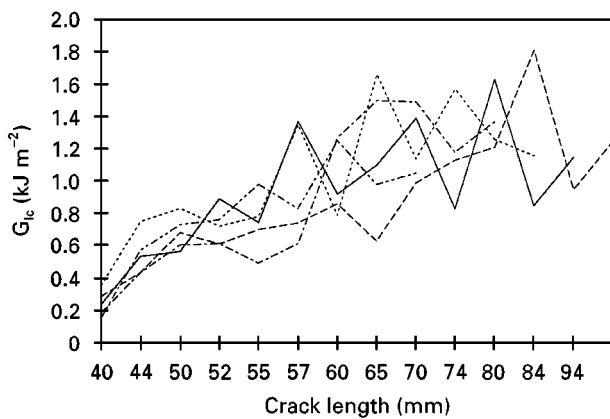


Figure 6 Mode-I, toughness G_{Ic} versus crack length for 5% Al-GFRP composites in dry and wet conditions. (—) $M_s = 0.85\%$; (---) $M_s = 0.96\%$; (····) $M_s = 1.15\%$; (-·-·) $M_s = 1.24\%$; (- - - -) $M_s = 0\%$.

of weight of filler content as shown in Figs 2 and 3. The results are based on the average value of three samples for each material. The results indicate that diffusivity coefficient and moisture content increased with increase of filler content. However, aluminium-tri-hydrate filled GFRP composites exhibited higher moisture content and diffusivity coefficient values than the polyethylene-filled GFRP composites. This is presumably due to the polar nature of the aluminium tri-hydrate particles and the relative particle size. Moisture gain in the interphase is believed to increase the modulus of the composite in that region by filling in the submicrocracks and voids and there is indication that microcracks formed in the conditioned materials (Fig. 4). The microcracking may be linked to differential swelling in fibre, particle and matrix phases and leaching of materials. Owing to the difference in elasticity and moisture expansion coefficients, stress develops along the glass fibre, particles and matrix interfaces. When these stresses exceed the adhesive fibre/particle/matrix bond strength, cracks may develop [4].

3.2. Water effects on toughness mode-I and mode-II

3.2.1. Toughness mode-I

The individual load–displacement curves for specimens tested in mode-I indicate that the specimens in all cases exhibit a well defined linear load–displacement relationship up to the point of crack initiation followed by a relatively well-behaved region of crack growth as shown in Fig. 5a to g. Crack propagation takes place by a series of regular small incremental jumps. It is possible to calculate a G_{Ic} value from the load at the onset of fracture and in addition, by using the area method (Equation 7) to assess G_{Ic} for each increment of crack growth. This latter method allows the generation of an *R*-curve linking G_{Ic} to crack length. In most cases e.g. Fig. 6, these plots of G_{Ic} versus crack length produce irregular curves which do tend towards a maximum value. The maximum and constant value of G_{Ic} from such a plot would be a suitable parameter to use to compare the

performance of the different materials. However, examination of the plots, typified by Fig. 6, reveals that deriving an upper limit for G_{Ic} would be a highly subjective operation for the results obtained in this work. Comparing trends between material compositions would be unsafe if based on this approach. Accordingly the effect of moisture content on mode-I toughness has been assessed by referring to the G_{Ic} values calculated from the maximum load at the point of crack initiation by the use of Equation 8.

Representative G_{Ic} values for each specimen data set are plotted against moisture content, as shown in Fig. 7a and b. It is interesting to note that in all cases, water immersion results in an increase in the measured fracture toughness. Indeed, the increase in toughness mode-I values for aluminium-tri-hydrate filled GFRP was up to 35%. Toughness increases in polyethylene-filled GFRP composites was only 13% at best with increases in the toughness of unfilled GFRP composites up to 20% after moisture uptake.

Mode-I, toughness values suggests that the amount of sub-microcracks and fibre bridging in particle filled and unfilled GFRP composites was greater than in their dry counterparts. An increase in the level of sub-microcracks and fibre bridging following water immersion may result from a weakening of the fibre–matrix, particle–matrix and fibre–particle interfacial strength, as can be identified from Fig. 8. Gaur *et al.* [2] showed that even very short periods of hydrothermal ageing reduced the interfacial shear strength of an E-glass/epoxy model composites system

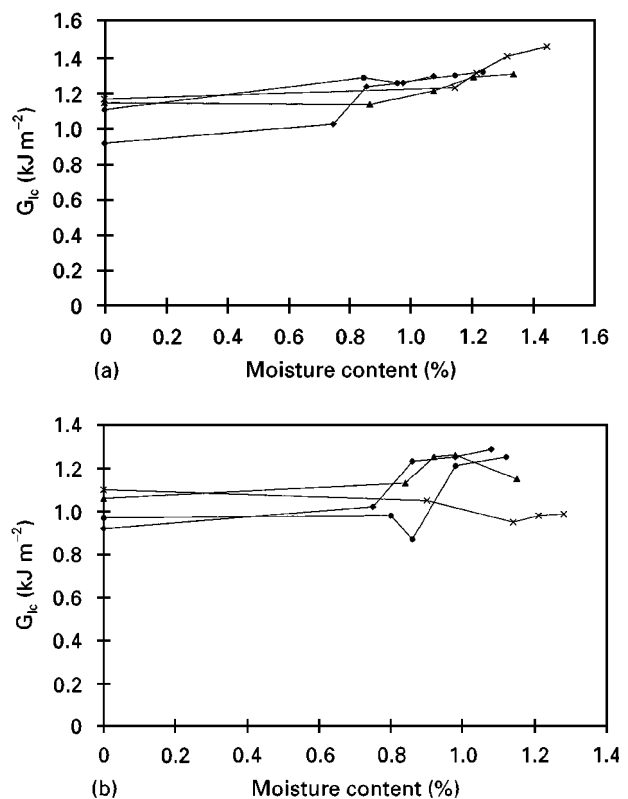


Figure 7 Mode-I toughness G_{Ic} versus moisture content for (a) GFRP and Al-GFRP composites (◆) GFRP; (●) 5% Al-GFRP; (▲) 10% PI-GFRP; (×) 15% Al-GFRP and (b) GFRP and PI-GFRP composites. (◆) GFRP; (●) 5% PI-GFRP; (▲) 10% PI-GFRP; (×) 15% PI-GFRP.

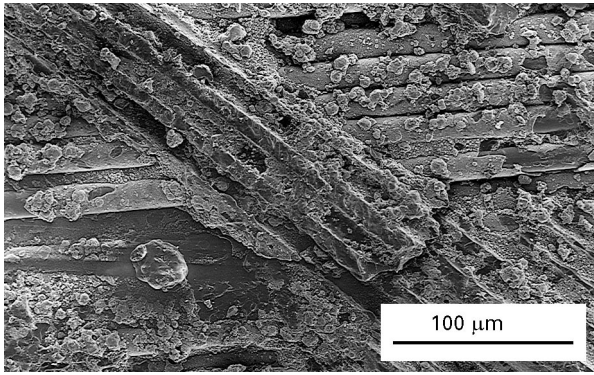


Figure 8 SEM micrograph showing matrix swelling and fibre debonding in particle-filled GFRP composites after immersion in water for 240 days at room temperature (20 °C).

by up to 40%. However, particle-filled composites exhibit increased sub-microcracks/fibre bridging, which proposes higher toughness values, as described earlier [13]. It is believed that the water ions are leached out of the glass by the aqueous environment, the matrix and particle swells and is plasticized and the physical primary bonds at the fibre/particle/matrix interface are weakened or destroyed. Selzer and Friedrich [14] attributed a 64% increase in the mode-I delamination toughness of a carbon fibre reinforced epoxy to a plastification of the matrix and increased fibre bridging. Similarly, Briscoe and Williams [15] conducted mode-I interlaminar fracture test on a series of Kevlar-reinforced epoxy composites and showed that laminates having low levels of fibre–matrix adhesion exhibited larger fibre bridging zones and offered higher values of G_{Ic} .

3.2.2. Toughness, mode-II

The effect of moisture content on the model-II, toughness, G_{IIc} , of unfilled GFRP is small, but a measurable increase in toughness from 1.25 kJ m^{-2} to 1.45 kJ m^{-2} was observed as shown in Fig. 9. The filled Al-GFRP specimens exhibited a somewhat higher mode-II toughness than GFRP before water and exposure this toughness rose further with increasing water content. The magnitude of this effect was somewhat irregular and was not consistent with filler content but was more closely linked to the initial magnitude of the unconditioned toughness. This may indicate that while a general increase in toughness can be attributed to water uptake, the absolute magnitude of the toughness is also influenced by factors such as material quality and the specific dispersion of filler in each sample. An increase in mode-II toughness in the GFRP and Al-GFRP composites is likely to be the result of microcracking and debonding of filler and fibres which will facilitate blunting at the crack tip. The specimens filled with polyethylene in contrast did not show any measurable increase in toughness after water uptake. Although the unconditioned composites had a higher toughness value than the corresponding Al-GFRP specimens, the values measured after water uptake fell back slightly to be similar or below the values recorded by conditioned Al-GFRP.

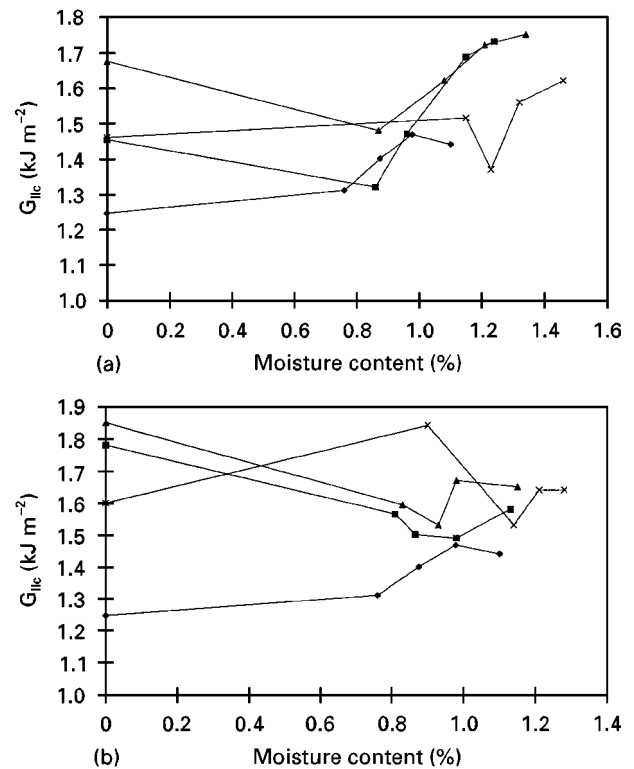


Figure 9 Mode-II toughness G_{IIc} versus moisture content in (a) GFRP and Al-GFRP composites (◆) GFRP; (■) 5% Al-GFRP; (▲) 10% Al-GFRP; (×) 15% Al-GFRP and (b) GFRP and PI-GFRP composites (◆) GFRP; (■) 5% PI-GFRP; (▲) 10% PI-GFRP; (×) 15% PI-GFRP.

This contrasting behaviour is likely to be caused by the fact that the polyethylene particles are not hydrophilic and there is little driving force encouraging the moisture to collect at the interface and debond the filler.

4. Conclusions

1. Increasing the filler content in GFRP composites resulted in increase in the equilibrium water uptake and an accompanying increase in the effective water diffusivity coefficient. However, aluminium-tri-hydrate filled GFRP composites resulted in higher content of moisture uptake and diffusivity coefficient than the polyethylene-filled and unfilled GFRP composites because of absorption of water to a greater extent.
2. The mode-I delamination toughness of all composites increased with increase of moisture content but changed little under mode-II.
3. Aluminium-tri-hydrate filled GFRP composite exhibit higher values of mode-I and mode-II than the polyethylene-filled and unfilled GFRP composites. It is clear that water immersion results in an increase in the delamination toughness in all of the composites. This absorbed water is attributed to the fibre–matrix, fibre–particle and particle–matrix interfaces resulting in increase submicrocracking and greater energy absorption after immersion.

Acknowledgements

This work was carried out at Department of Materials, Queen Mary & Westfield College, University of

London, Mile End Road, London, E1 4NS, UK with the financial support of the British Council, London, UK. One of us (V. K. Srivastava) was the recipient of a Commonwealth Academic Staff Fellowship.

References

1. W. J. CANTWELL, G. BROSTER and P. DAVIES, *J. Reinf. Plast. Comp.* **15** (1996) 1161.
2. U. GAUR, C. T. CHOU and B. MILLER, *Composites* **25** (1994) 609.
3. A. J. RUSSEL and K. N. STREET, "Moisture and temperature effects on the mixed-mode delamination, fracture of unidirectional graphite/epoxy, delamination and debonding of materials", ASTM STP-876, edited by W. S. Johnson (American Society for Testing and Materials, Philadelphia, 1985) p. 349.
4. T. S. GRANT and W. L. BRADLEY, *J. Comp. Mater.* **29** (1995) p. 852.
5. W. J. EAKIN "Effect of water on glass fibre resin bonds, interfaces in composites", ASTM STP-452 (American Society for Testing and Materials, Philadelphia, 1969) p. 137.
6. A. LEKATOU, S. E. FAIDI, D. GHIDAQUI, S. B. LYON and R. C. NEWMAN, *Composites, A* **28A** (1997) 223.
7. C. SOUTIS and D. RURKMEN, *J. Comp. Mater.* **31** (1997) 832.
8. Y. ARSLANIAN and P. J. HOGG, "Measurement of stress corrosion crack growth in sheet moulding compounds, high temperature and environmental effect on polymeric composites, ASTM-1174 (American Society for Testing and Materials, Philadelphia, 1993) p. 7.
9. C. H. SHEN and G. S. SPRINGER, *J. Comp. Mater.* **10** (1976) 1.
10. J. JHOU and J. P. LUCAS, *Comp. Sci. Technol.* **53** (1995) 57.
11. V. K. SRIVASTAVA and B. HARRIS, *J. Mater. Sci.* **31** (1994) 548.
12. H. J. SUE, J. E. JONES and E. I. GARICA-MEITIN, *ibid.* **28** (1993) 6381.
13. V. K. SRIVASTAVA and P. J. HOGG, *ibid.* **33** (1998) 1119.
14. R. SELZER and K. FRIEDRICH, in Proceedings of ICCM-9, edited by A. Miravete (Woodhead, Publishers, Cambridge, 1993) p. 875.
15. B. J. BRISCOE and D. R. WILLIAMS, *Comp. Sci. Technol.* **46** (1993) p. 227.

*Received 11 September
and accepted 23 October 1997*